Modeling Dark Energy

Gravimetric analysis of a tensegrity icosahedron simulates universal accelerated expansion

Robert G. Chester
Tumwater, WA
N914TJ (at) comcast (dot) net

Abstract

Tensegrity structures exhibit several counterintuitive behaviors. Among these is expansion resulting solely from internal tension. Replacing the physical tendons of a six-strut tensegrity icosahedron with classical gravitational attraction suggests that universal accelerated expansion may be due to ordinary gravity acting solely as an inverse second-power attractive force. Speculation is included on the ultimate fate of the universe.

Key words: Dark Energy, Fuller, Gravity, Tensegrity

1.0 Introduction

The accelerated expansion of the universe has been of intense interest to astronomers since its discovery in 1998 [1, 2]. Attempts to explain this phenomenon have included string theory [3, 4, 5, 6], football−shaped extra dimensions and branes [7], and geometric models of Quintessence [8]. Many authors propose that negative or repulsive gravity is the cause of the observed acceleration [9, 10, 11, 12, 13, 14, 15, 16]. The favored explanation so far seems to be Einstein's Cosmological Constant, or what Padmanabhan calls "the weight of the vacuum" [17].

This paper explores another hypothesis entirely. A tensegrity icosahedron, when analyzed gravimetrically, spontaneously expands under the influence of nothing more than classical gravity, suggesting that ordinary gravity, acting solely as an inverse second power attractive force, may be capable of producing the accelerated expansion of the universe. The argument is based on principles embodied in Buckminster Fuller's patented structural system, tensegrity [18].

2.0 The tensegrity icosahedron

The simplest example of a spherically symmetric tensegrity structure is the tensegrity icosahedron [19].

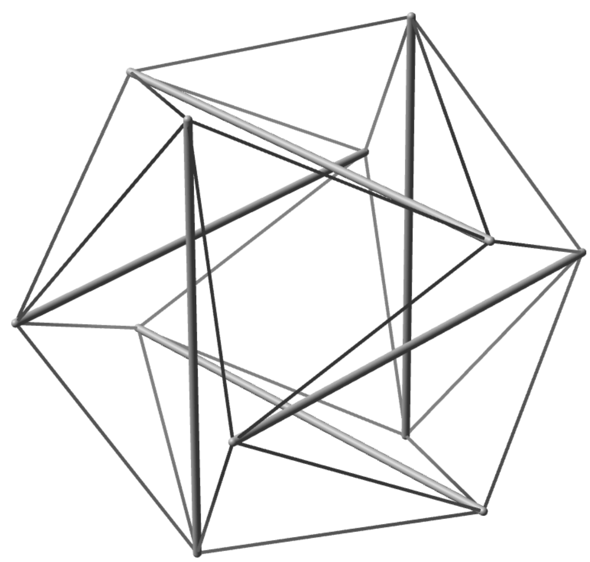

Fig. 2.0.1. The tensegrity icosahedron [20]

The tensegrity icosahedron is composed of six identical compression struts linked by 24 identical tension members. The compression struts are arrayed in parallel pairs, two in each of the three Cartesian planes. Each compression strut is attached to eight tension members. Four of these tendons result in a force radially outward. The other four result in a force radially inward. Of particular note is the fact that any given tendon has force components directed both inward and outward. In other words, if the compression strut at one end of the tendon experiences a force component inward, then the strut at the other end of the tendon experiences a force component outward. Tension stabilizes the system by exerting simultaneous inward and outward forces. All forces are balanced and the system is in equilibrium.

Icosahedra have 12 vertices, 20 faces, and 30 edges. Although the tension members of the tensegrity structure trace the edges of the icosahedron, the present structure has only 24 tension members. Six of the icosahedral edges are missing. The six missing edges bridge the valleys in which the compression struts are suspended. Like all tensegrity structures, the tensegrity icosahedron displays continuous tension and discontinuous compression. Remote compression struts are suspended in an integral tension net. None of the compression members touches any other, and yet the structure is stable. The tension net holds the discrete compression members suspended in space.

One may suppose that the tensegrity icosahedron is a static structure, but it is not. Physical tendons are always in some measure elastic. They stretch or contract to accommodate the forces they carry. Furthermore, the variable length of the tendons relates directly to the radius of the icosahedron. We will next compare the radius with the length of the tendons.

2.1 The radius of the tensegrity icosahedron

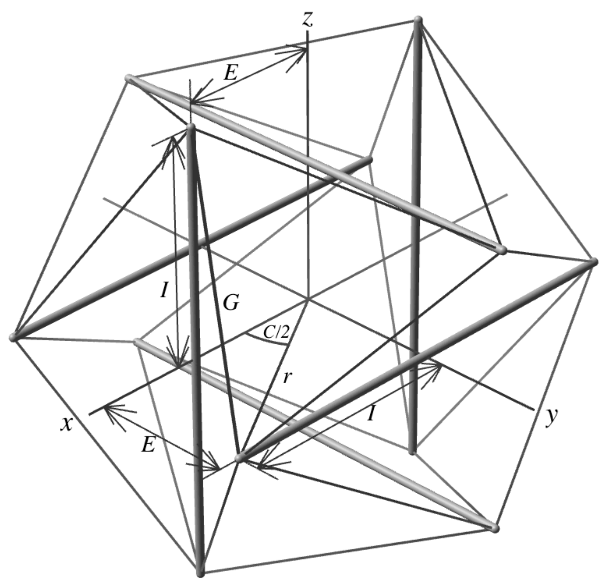

Fig. 2.1.1. Tensegrity icosahedron with Cartesian axes

In Fig. 2.1.1 the tensegrity icosahedron is centered on the Cartesian coordinate system. The positive *x* axis bisects a vertical compression strut. The strut is parallel to the *z* axis and at a distance *E* from it. The half strut length is *I*. This description applies to all six of the compression struts: all six are located at a distance *E* from the corresponding parallel axis, and the half strut length of each is *I*. One of the tendons is labeled *G*. A unit radius, *r*, is drawn in the xy-plane. 2E subtends angle C (not shown), which is the central angle subtended by an edge of the regular icosahedron. Kenner [21] points out that in the regular icosahedron

$$C = \operatorname{atan} 2. \tag{1}$$

The unit radius makes an angle of C/2 with the *x* axis. Thus

$$E = \sin\frac{C}{2}, \tag{2}$$

$$I = \cos\frac{C}{2}, \tag{3}$$

and

$$r = \sqrt{I^2 + E^2}. \tag{4}$$

However, although the half strut length I is fixed, the distance E of the compression struts from the origin is not. Due to the elasticity of the tendons, the compression struts may move toward or away from the center of the system [22]. (For this analysis we will ignore rotational effects.) Thus the radius is also variable:

$$r = \sqrt{I^2 + (xE)^2}. \tag{5}$$

A radius to any vertex may be expressed in a similar manner. Equation (5) is therefore a general expression for all radii of the structure. That is, all radii will expand or contract equally when the distance of the compression struts from their parallel axes changes [23].

2.2 The length of the tendons of the tensegrity icosahedron

Again with reference to Fig. 2.1.1, the length of tendon G is

$$G = \sqrt{(I-E)^2 + E^2 + (-I)^2}. \tag{6}$$

But G, like the radius, must vary with x:

$$G = \sqrt{(I-xE)^2 + (xE)^2 + I^2}. \tag{7}$$

Since any tendon has the same relationship to the coordinate axes, equation (7) is a general expression for the length of any G tendon of the structure.

Graphing G and r with respect to x,

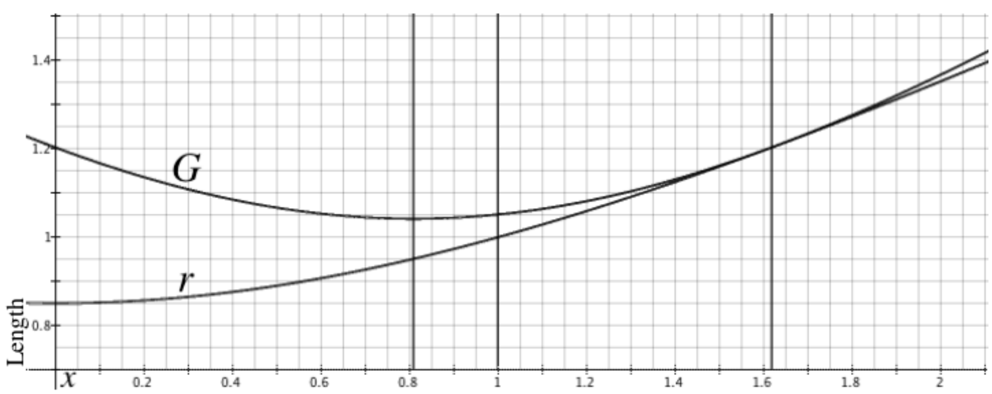

Fig. 2.2.1. The radius compared to the length of the tendons

Figure 2.2.1 compares G, the length of the tendons, with the radius of the tensegrity. On the right the curves are tangent at $x = 1.62\ldots(2 \cos 36^\circ)$ [24]. At $x = 1.00$ the radius is 1.00 while the tendon length is 1.05… which is the length of the edge of a regular icosahedron with a unit radius.

The minimum tendon length occurs at $x = 0.809\ldots$ (cos 36˚) where $r = 0.951\ldots$ and $G = 1.04\ldots$. The difference between the minimum tendon length and the edge of a regular icosahedron is about 1%, while the radius changes by slightly less than 5%.

The graph shows that elastic tendons in a six strut icosahedral tensegrity will seek a minimum length. Beginning where the curves are tangent and reading the graph from right to left, the tendons draw in the structure until the they achieve their minimum length. The graph can also be read left to right. If $0.0 < x < \cos 36^\circ$, then the tendons will pull the compression struts outward to equilibrium. The radius increases and the structure gets larger, but the tendons are contracting, and will continue to do so until they again reach their minimum length. Since the tendons are stressed solely in tension, in this interval it is tension alone that causes the expansion. All tensegrity structures share this behavior. When disturbed, they have an equilibrium radius toward which they will expand or contract.

The tensegrity model suggests an explanation for the observed accelerated expansion of the universe. Tension alone is sufficient to expand a physical system as well as to cause it to contract. Tension alone is sufficient to increase a tensegrity system's radius as well as to decrease it. But desktop systems are not the physical universe. In order to explore the behavior of the tensegrity icosahedron when the physical tendons are replaced by gravity, four aspects of the model need to be modified.

3.0 Modifying the model

The physical tensegrity model differs from that proposed for gravimetric analysis. First, masses in the real world attract and are attracted by all other masses, whereas in the tensegrity model each compression strut is directly linked to only four of the five other struts in the structure; parallel struts are not connected. Second, the tendons of the physical model attach to the compression struts only at the ends, but when considered gravimetrically, any given strut must attract each and every other strut along their entire lengths. Third, the elastic tendons follow Hooke's Law, not the inverse squared law of gravity, and fourth, conventional analysis indicates that masses that experience the mutual attraction of gravity will move toward each other. The idea that masses can be mutually attracted toward each other and still move apart is unknown. Each of these points will be dealt with in turn.

3.1 Connecting the dots

The first modification needed to convert the physical tensegrity to the gravimetric model relates to the fact that masses in the real world attract and are attracted by all other masses, whereas in the tensegrity model each compression strut is tensionally linked to only four of the five other struts. The solution is to connect everything to everything else.

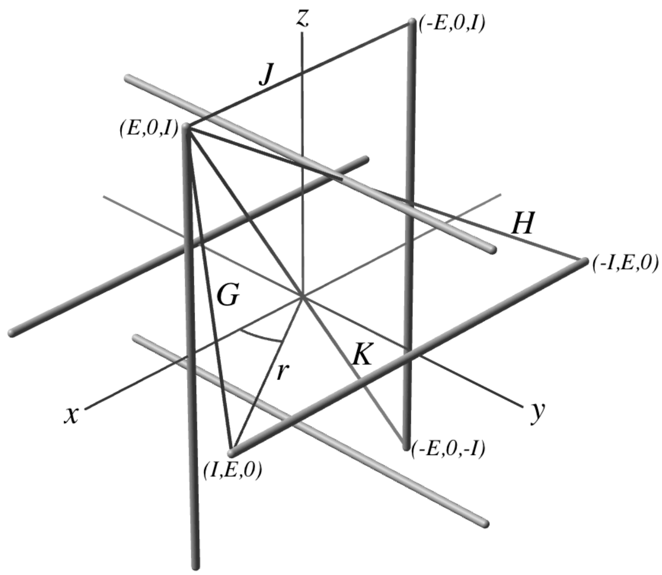

Fig. 3.1.1. The four chordal relationships of the tensegrity icosahedron

Shown here in the original configuration of Fig. 2.1.1 are the six compression struts of the tensegrity icosahedron. Four exemplar chords *G*, *H*, *J*, & *K* illustrate the four-and-only four relationships of point (*E*,0,*I*) to each of the other struts. Beginning with the *G* chord, this and twenty three more like it stabilize the structure by pulling the compression struts simultaneously inward and outward.

An *H* chord extends from (*E*,0,*I*) to (–*I*,*E*,0). Like the *G* chords, there are 24 *H* chords. Their net effect on the structure is as yet undetermined.

The tensegrity icosahedron in Fig. 2.1.1 is missing six of its icosahedral edges. Although the missing edges were previously mentioned briefly and then dismissed, they represent real relationships and must now be taken into account. A *J* chord extends from (*E*,0,*I*) to (–*E*,0,*I*). It represents the missing icosahedral edges. There are six such chords.

Finally a *K* chord connects (*E*,0,*I*) to (–*E*,0,–*I*) through the center of the system. There are two diameters in each of the Cartesian planes, forming an X between the opposite ends of parallel compression struts. All told, there are six of these chords. Sumtotally, there are 24 + 24 + 6 + 6 = 60 chordal relationships that need to be considered.

The length of the *G* chord with respect to *x* was previously found to be

$$G = \sqrt{(I - xE)^2 + (xE)^2 + I^2} . \tag{7}$$

Similarly, the lengths of the *H*, *J*, and *K* chords may be expressed as

$$H = \sqrt{(I + xE)^2 + (xE)^2 + I^2} , \tag{8}$$

$$J = \sqrt{(2xE)^2}, \tag{9}$$

and

$$K = \sqrt{(2xE)^2 + (2I)^2}. \tag{10}$$

The radius is still

$$r = \sqrt{I^2 + (xE)^2}. \tag{11}$$

Graphing G, H, J, K, and r with respect to x yields

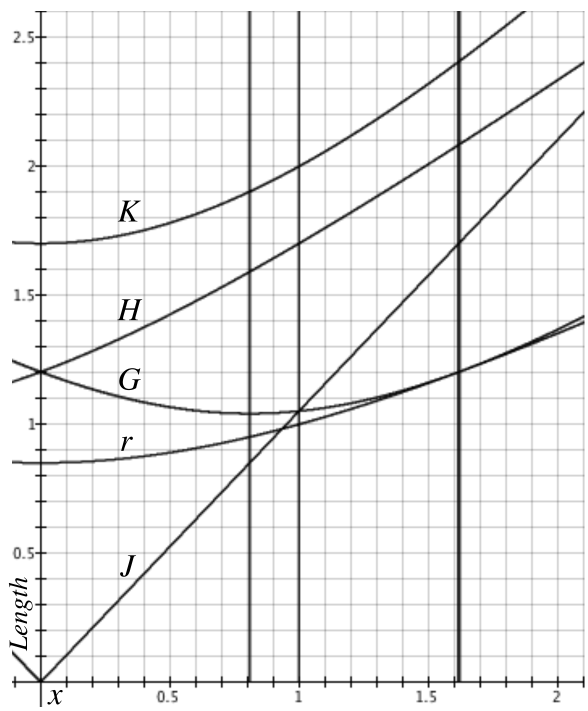

Fig. 3.1.2. The radius compared to the lengths of the four chord families

In figure 3.1.2 we again note the tangency of the G and r curves at $x = 1.62\ldots$, the regular icosahedron at $x = 1.00$, and the minimum of the G curve at $x = 0.809\ldots$. The graph also reveals that although the G and J chords are both edges of the icosahedron, $G = J$ only at the regular icosahedron, $x = 1.00$.

In figure 2.2.1 it was found that the G chords tend to pull the structure outward to equilibrium if $0.00 < x < \cos 36^\circ$. Now the situation is more complex. The present graph shows that, in this same interval, the H, J, and K chords all work in opposition to the G chords. That is, whereas the G chords tend to expand the structure in the interval $0.00 < x < \cos 36^\circ$, the others tend to cause it to collapse. Elsewhere, i.e. $\cos 36^\circ < x$, all four chord types tend to contract the tensegrity and reduce its radius.

3.2 Extended bodies

The second modification needed to prepare the tensegrity icosahedron for gravimetric analysis is the fact that the tendons of the physical model attach to the compression struts only at the ends, but when considered gravimetrically, any given strut must attract each and every other strut along their entire lengths.

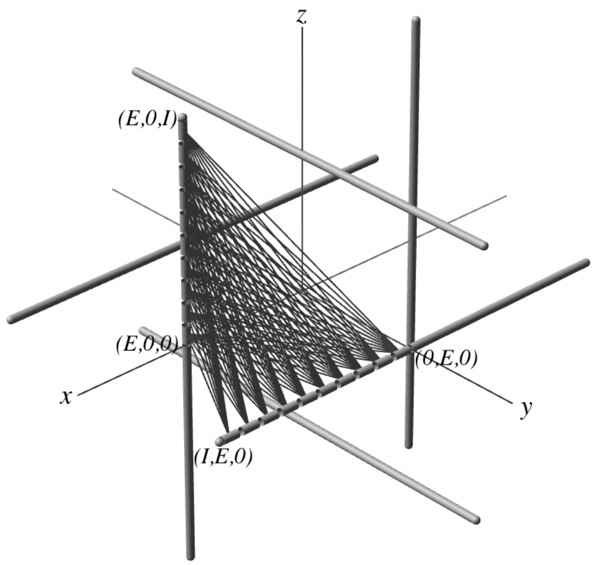

Fig. 3.2.1. The 100 *Gn* chords

To approximate the attraction of extended bodies, the half struts at (*E*,0,0) - (*E*,0,*I*) and (0,*E*, 0) - (*I*,*E*,0) are divided into 10 sections. Each section of each half strut is then connected to every section of the other half strut forming 100 *Gn* chords. This results in a set of 100 equations of the form [25]

$$G_n = \sqrt{\left(\frac{G_x}{20}I - xE\right)^2 + (xE)^2 + \left(-\frac{G_z}{20}I\right)^2} \qquad (12)$$

where

n: 1 —> 100,

and

$$G_x = G_z = \{1, 3, 5, 7, 9, 11, 13, 15, 17, 19\}.$$

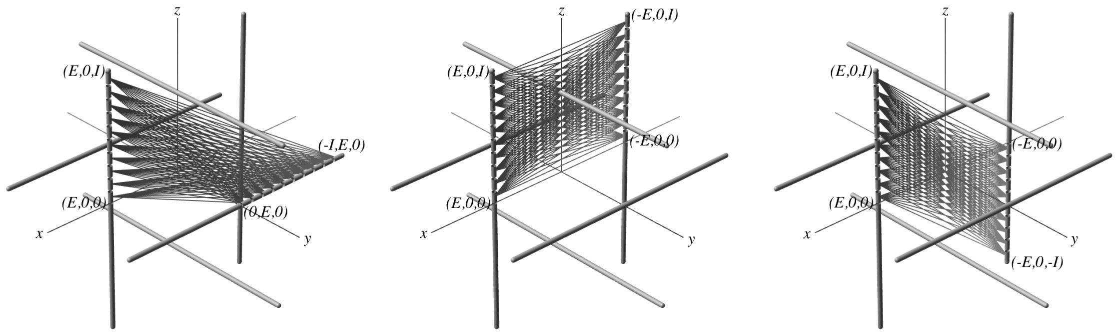

Hn *Jn* *Kn*

Fig. 3.2.2. The 100 each *Hn*, *Jn*, and *Kn* chords

Similarly, the original *H*, *J*, and *K* chords may be converted into 100 each *Hn*, *Jn*, and *Kn* chords by subdividing the original half struts.

3.3 Hooke to Newton

The third difference between the tensegrity model and the larger world is that elastic tendons follow Hooke's Law rather than the inverse second power law of gravity. The modification needed is a straightforward application of Newton's law of universal gravitation.

$$F = \mathbf{G}\frac{m_1 m_2}{d^2} \tag{13}$$

For purposes of this discussion the gravitational constant and the masses may be omitted. These add scale, but do not materially change the inverse second power relationship. Thus the relative force between any two centers of mass may be written as

$$F = \frac{1}{d^2}. \tag{14}$$

The total gravitational force, *F*, of the T−icosa will be the algebraic sum of the gravitational forces from each of the T−icosa's 60 chordal relationships. However, before making this calculation we need to rethink mutual attraction.

3.4 A new rule of mutual attraction

The last challenge faced by the tensegrity model is the fact that under conventional analysis bodies that experience the mutual attraction of gravity are expected to move toward each other [26, 27]. The idea that bodies can undergo mutual attraction and still move apart is unknown. Furthermore, even though the distance between the bodies is without exception expected to decrease, the force of attraction is conventionally given a positive sign. In contrast, the tensegrity model allows the distance between bodies to increase or decrease under the influence of gravity. A new rule is needed.

When gravity increases or tends to increase the distance between masses, it will be given a positive sign. When it decreases or tends to decrease the distance between masses, it will be given a negative sign.

It is critical to emphasize immediately that this new rule does not define or imply “negative gravity.” The tensegrity model posits only an attractive force, but specifying the net effect of that force is of central importance. Although this rule modifies the conventional treatment of gravity as always having a positive sign, there is a precedent. In astronomy, objects which are receding from the observer at a velocity great enough for their light to be shifted toward the red end of the spectrum are said to be redshifted. The distance between observer and observed is increasing, and the redshift is given a positive sign. On the other hand, when objects are approaching the observer fast enough for their light to be shifted toward the blue end of the spectrum, the distance between observer and observed is decreasing, and the redshift is given a negative sign [28]. The tensegrity model adopts this astronomical usage.

This new view avoids the terms “negative pressure” [29, 30, 31, 32, 33, 34, 35], “negative energy density” [36], “repulsive gravity” [37, 38, 39], “repulsive fixed point” [40], “repulsive gravitational effects” [41], and so on. The tensegrity model stipulates a single kind of gravity. It is attractive in nature and tends to reduce the distance between individual masses. Even so, there are two distinct effects of mutual attraction. While the distance between individual masses may be reduced, the system composed of such masses may either expand or contract.

The total gravitational attraction, F_G, due to the 100 *Gn* chords is therefore

$$F_G = G_1+G_2+G_3+\ldots+G_{98}+G_{99}+G_{100}.$$

Similarly, the total gravitational attraction due to the 100 F_H, F_J, and F_K chords will be expressed as

$$F_H = H_1+H_2+H_3+\ldots+H_{98}+H_{99}+H_{100},$$

$$F_J = J_1+J_2+J_3+\ldots+J_{98}+J_{99}+J_{100},$$

and

$$F_K = K_1+K_2+K_3+\ldots+K_{98}+K_{99}+K_{100}.$$

4.0 Gravimetric analysis of the tensegrity icosahedron

It was found previously that the length of the *Gn* chords is

$$G_n = \sqrt{\left(\frac{G_x}{20}I - xE\right)^2 + (xE)^2 + \left(-\frac{G_z}{20}I\right)^2} \tag{12}$$

Substituting into the force expression (14), yields

$$F_G = \frac{1}{\left(\frac{G_x}{20}I - xE\right)^2 + (xE)^2 + \left(-\frac{G_z}{20}I\right)^2}. \tag{15}$$

And, since there are 24 of them,

$$F_G = \frac{24}{\left(\frac{G_x}{20}I - xE\right)^2 + (xE)^2 + \left(-\frac{G_z}{20}I\right)^2}. \tag{16}$$

Similarly, the forces due to the *H*, *J,* and *K* chords are

$$F_H = \frac{24}{\left(-\frac{H_x}{20}I - xE\right)^2 + (xE)^2 + \left(-\frac{H_z}{20}I\right)^2}, \tag{17}$$

$$F_J = \frac{6}{(-2xE)^2 + \left(\frac{J_z}{20}I\right)^2}, \tag{18}$$

and

$$F_K = \frac{6}{(-2xE)^2 + \left(-\frac{K_z}{20}I\right)^2}. \tag{19}$$

We know from Figs. 2.2.1 & 3.1.2 that the *G* chords can either move the compression struts inward, toward the center of the system, or outward, away from the center of the system. The question is, what are the signs of the force expressions? Because the universe is currently expanding, F_G will be considered positive. On the other hand, Fig. 3.1.2 shows that the *H*, *J*, and *K* chords all work in a manner opposed to the *G* chords. Thus F_H, F_J, and F_K all receive a negative sign. The total gravitational force, *F*, of the tensegrity icosahedron is therefore

$$F = F_G - F_H - F_J - F_K. \tag{20}$$

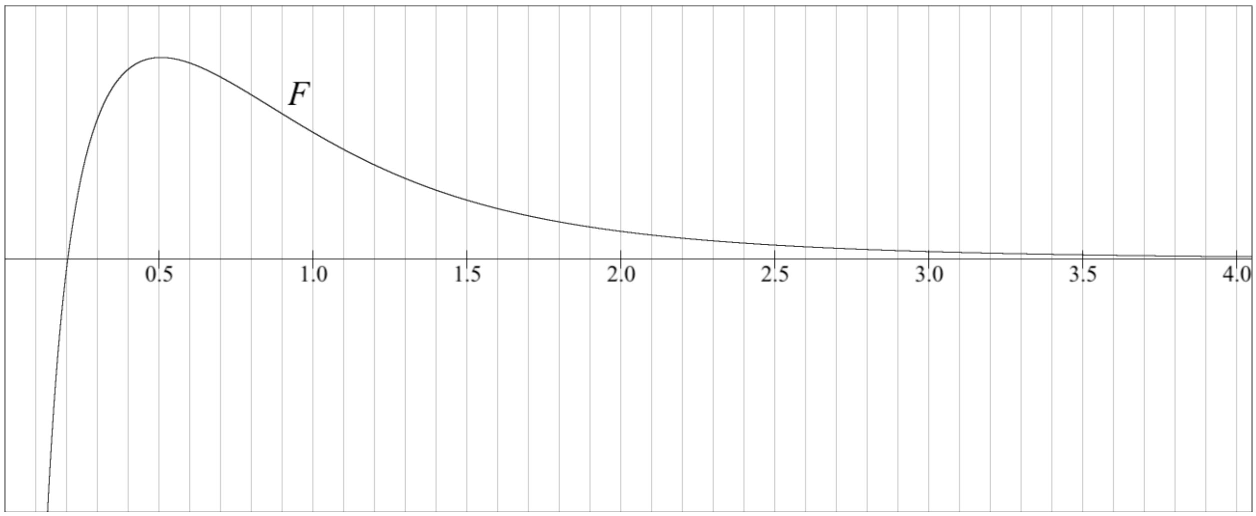

Fig. 4.0.1a. Total gravitational force of the tensegrity icosahedron

Figure 4.0.1a displays the algebraic sum, F, of the gravitational forces of the tensegrity icosahedron with respect to x. When $y < 0$, gravity reduces or tends to reduce the distance between the compression struts, and the tensegrity icosahedron contracts. When $0 < y$, the effect is to increase the distance between the struts, and the structure expands. At $x = 0.00$ the total force diverges contractively without limit. There is an x axis intercept at $x = 0.204\ldots$, and a maximum at $x = 0.507\ldots$. The total force, still expansive, then decreases and appears to approach the x axis asymptotically from the positive direction, but in fact it intersects the axis again at $x = 6.40\ldots$. The graph reaches a local minimum at $x = 9.65\ldots$, and only after that does it slowly increase to approach the x axis asymptotically from the contractive direction.

Although it is apparent that the curve diverges negatively without limit at $x = 0.00$, the maximum y value at $x = 0.507\ldots$ and the local minimum at $x = 9.65\ldots$ are not specified because the force equation (14) is relative, not absolute. It omits the masses of the compression struts as well as the gravitational constant $\mathbf{G}$.

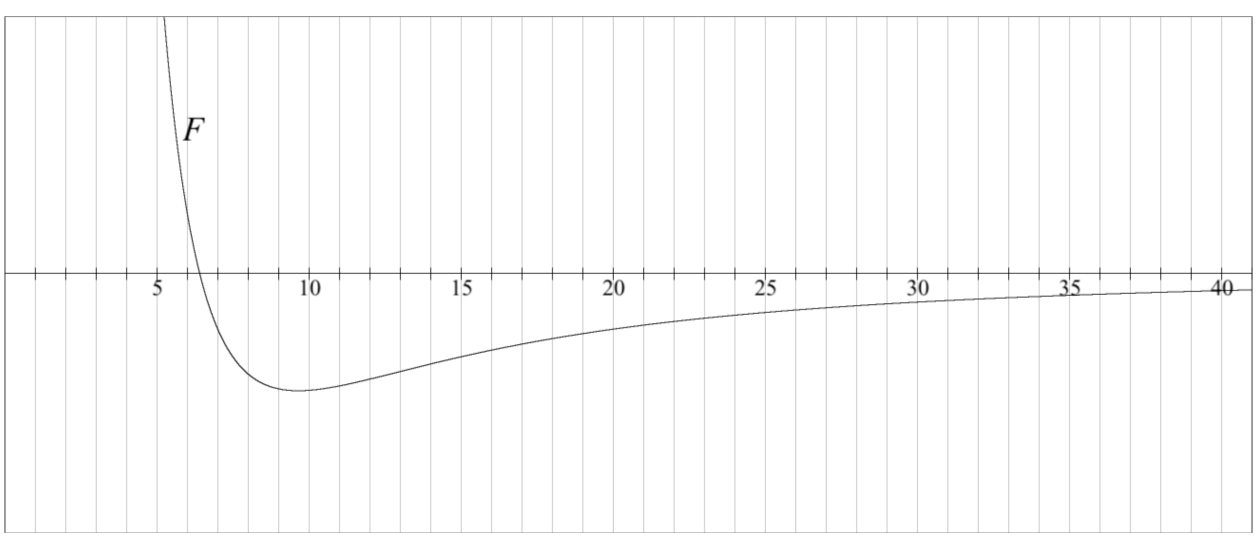

Fig. 4.0.1b. Detail: total gravitational force of the tensegrity icosahedron

By expanding the y axis by a factor of 5 x 10^2, and collapsing the x axis by a factor of 5.00, Fig. 4.0.1b shows a second x axis intercept at $x = 6.40\ldots$, the gravitational minimum at $x = 9.65\ldots$, and a slow recovery towards – but never reaching – equilibrium.

Riess et al. report that their data are "… consistent with a currently accelerating expansion…" [42]. The tensegrity model supports this conclusion in the interval $0.204 \leq x \leq 6.40\ldots$ when the effect of the total gravitational force is to accelerate the observed expansion. However in that same paper the investigators report that, "The data favor eternal expansion as the fate of the universe…." In contrast, the tensegrity model suggests that the total gravitational force driving the current accelerated expansion will increase to a maximum, then decrease until it is slightly compressive, and only then asymptotically approach equilibrium. Like all tensegrity structures, the model suggests that the universe will expand to a very large but finite size, then contract slowly, with the rate of contraction slowing with time until it's imperceptible — a cosmic bounce, if you will.

5.0 Discussion

A model based on Fuller's six strut tensegrity icosahedron has been developed, and the interplay of gravitational forces it generates has been calculated. What can be said for now is that when the physical tendons are replaced with gravitational forces there appears to be an interval, $0.204\ldots < x < 6.40\ldots$, where the structure will spontaneously expand. The question remains, is the universe a tensegrity? Fuller defines tensegrity as

> …a structural-relationship principle in which structural shape is guaranteed by the finitely closed, comprehensively continuous, tensional behaviors of the system, and not by the discontinuous and exclusively local compressional member behaviors… All structures, properly understood, from the solar system to the atom, are tensegrity structures. Universe is omnitensional integrity [43].

He goes on to say

> [Tensegrity] explains why it is that all local celestial systems of Universe, being cohered with one another tensionally, pull on one another to bring about an omniexpanding physical Universe [44].

Fuller intuited the relationship between the tensegral nature of the universe and expansion, although it's not clear from the above whether he saw the expansion as accelerated. Nevertheless, the tensegrity model suggests that gravity, acting solely as an inverse second power attractive force, can cause the observed accelerated expansion of the universe. Fig. 4.0.1a suggests expansion will occur in the interval $0.204\ldots \leq x \leq 6.40\ldots$, with the maximum acceleration at $x = 0.507...$ and decreasing thereafter. The limit of accelerated expansion occurs at $x = 6.40\ldots$ when the force curve intersects the x axis and becomes contractive.

5.1 Uniqueness of the tensegrity model

The tensegrity model enjoys one feature that is unique to it alone: There exists a desktop physical system such as that in Fig. 2.0.1 that behaves precisely as shown in Fig. 2.2.1. This counterintuitive behavior has been observed only in tensegrity structures.

5.2 Going forward

There exist at least two avenues for further exploration of the relationship of tensegrity to dark energy. First, the six strut tensegrity investigated here is but one of an infinite family of omnisymmetrical tensegrities [45]. More struts may be added without limit. Furthermore, tensegrity structures may employ not only increased numbers of struts in a single, thin-shell configuration, but additional shells may be added without limit. The behaviors of multi-strut multi-shell Tensegrities may more closely model the observed accelerated expansion of the universe than the current model. Second, a Cavendish-like experiment [46] might quickly resolve the question of tensegrity structures' relationship to the accelerated expansion of the universe.

6.0 Acknowledgments

I must first and foremost recognize the profound creativity of Buckminster Fuller, without whom this paper would not exist. His recorded wisdom and insights have been crucial at every juncture. Also, I must acknowledge the contributions of Freeman Dyson, who provided helpful comments on an early version of this paper. That said, whatever the merits or failures of the work may be, they are the responsibility of the author alone. Finally, let me state that the current work was not supported by any group, funding body, or individual other than the author himself.

1 Perlmutter et al. 1998. (The Supernova Cosmology Project) *Measurements of Omega and Lambda from 42 high redshift supernovae*. arXiv:astro-ph/9812133.

2 Riess et al. 1998. *Observational Evidence from Supernovae for an Accelerating Universe and a Cosmological Constant*. arXiv:astro-ph/9805201.

3 Carroll. 2000. *The Cosmological Constant*. arXiv:astro-ph/0004075.

4 Padmanabhan. 2003. *Cosmological Constant – The Weight of the Vacuum*. arXiv:hep-th/0212290.

5 Peebles et al. 2002. *The Cosmological Constant and Dark Energy*. arXiv:astro-ph/0207347.

6 Trodden. 2007. *Theoretical Approaches to Cosmic Acceleration*. arXiv:gr-qc/0702081.

7 Carroll et al. 2003. *Is Cosmic Speed-Up Due to New Gravitational Physics*? arXiv:astro-ph/0306438.

8 Folomeev et al. 2007. *Geometric Model of Quintessence*. arXiv:astro-ph/0701375.

9 Carroll. 2000. The Cosmological Constant. arXiv:astro-ph/0004075.

10 Carroll et al. 2003. *Sidestepping the Cosmological Constant with Football-Shaped Extra Dimensions*. arXiv:hep-th/0302067.

11 Huterer et al. 1999. *Prospects for probing the dark energy via supernova distance measurements*. arXiv:astro-ph/9808133.

12 Padmanabhan. 2003. *Cosmological Constant – The Weight of the Vacuum*. arXiv:hep-th/0212290.

13 Peebles et al. 2002. *The Cosmological Constant and Dark Energy*. arXiv:astro-ph/0207347.

14 Riess et al. 1998. *Observational Evidence from Supernovae for an Accelerating Universe and a Cosmological Constant*. arXiv:astro-ph/9805201.

15 Riess et al. 2004. *Type Ia Supernova Discoveries at $z > 1$ from the Hubble Space Telescope: Evidence for Past Deceleration and Constraints on Dark Energy Evolution*. AstroP J, 607:665-87.

16 Riess et al. 2006. *New Hubble Space Telescope Discoveries of Type Ia Supernovae at $z \geq 1$: Narrowing Constraints on the Early Behavior of Dark Energy*. arXiv:astro-ph/0611572.

17 Padmanabhan. 2003. *Cosmological Constant – The Weight of the Vacuum*. arXiv:hep-th/0212290.

18 U.S. Pat. 3,063,521.

19 Kenner (1976, p. 11) notes that "spherically symmetric" in this context means that when the face patterns [of the tensegrity icosahedron] are projected onto a sphere, they divide the surface of the sphere into symmetrically placed zones.

20 The illustrations in this paper are generated with Graphing Calculator by Pacific Tech www.PacificT.com/. Macintosh and PC versions are available. Instructions for making this structure may be found at www.youtube.com/watch?v=8gtvxYZ0GIg.

21 Kenner, H. 1976, *Geodesic Math and How To Use It*. University of California Press, Berkeley, pp. 126-136.

22 An illustration of this behavior can be found at https://www.youtube.com/watch?v=kAVfislbocY.

23 Equal and simultaneous expansion on all axes is also a characteristic of the Hoberman Sphere. However, this expansion is not powered internally. The applied force must be external to the Sphere.

24 Readers may recognize this number as the Golden Ratio.

25 Division by 20 in equation (12) arises from the fact that there are 20 half-sections in each half strut.

26 Guth, A. H. 1997, *The Inflationary Universe*. Helix Books, an imprint of Addison-Wesley Publishing Company, Inc., Reading, MA, Appendix A.

27 Randall, L. 2011, *Knocking on Heaven's Door – How physics and scientific thinking illuminate the universe and the modern world*. HarperCollins, New York, p. 372.

28 Peebles, P. J. E., & Ratra, B. 2003, Rev.Mod.Phys.75:559-606,2003, n. 35. (also available at astro-ph/0207347v2)

29 Carroll. 2000. *The Cosmological Constant*. arXiv:astro−ph/0004075.

30 Carroll et al. 2003. *Is Cosmic Speed−Up Due to New Gravitational Physics?* arXiv:astro−ph/0306438.

31 Huterer et al. 1999. *Prospects for probing the dark energy via supernova distance measurements*. arXiv:astro−ph/9808133.

32 Peebles et al. 2002. *The Cosmological Constant and Dark Energy*. arXiv:astro−ph/0207347.

33 Riess et al. 1998. *Observational Evidence from Supernovae for an Accelerating Universe and a Cosmological Constant*. arXiv:astro−ph/9805201.

34 Riess et al. 2004. *Type Ia Supernova Discoveries at $z > 1$ from the Hubble Space Telescope: Evidence for Past Deceleration and Constraints on Dark Energy Evolution*. AstroP J, 607:665−87.

35 Riess et al. 2006. *New Hubble Space Telescope Discoveries of Type Ia Supernovae at $z \geq 1$: Narrowing Constraints on the Early Behavior of Dark Energy*. arXiv:astro−ph/0611572.

36 Padmanabhan. 2003. *Cosmological Constant – The Weight of the Vacuum*. arXiv:hep−th/0212290.

37 Bojowald. 2008. *Loop Quantum Cosmology*. Living Rev. Relativity, 11, (2008), 4. http://www.livingreviews.org/lrr−2008−4 Accessed 2008 Sep 20.

38 Padmanabhan. 2003. *Cosmological Constant – The Weight of the Vacuum*. arXiv:hep−th/0212290.

39 Riess et al. 2006. *New Hubble Space Telescope Discoveries of Type Ia Supernovae at $z \geq 1$: Narrowing Constraints on the Early Behavior of Dark Energy*. arXiv:astro−ph/0611572.

40 Carroll. 2000. *The Cosmological Constant*. arXiv:astro−ph/0004075.

41 Padmanabhan. 2003. *Cosmological Constant – The Weight of the Vacuum*. arXiv:hep−th/0212290.

42 Riess, A. G., et al. 1998, Astron.J.116:1009-1038,1998. (also available at astro-ph/9805201v1)

43 Fuller, R. B. 1975, *Synergetics – Explorations in the Geometry of Thinking*. Macmillan, New York, p. 372.

44 Fuller, R. B. 1975, *Synergetics – Explorations in the Geometry of Thinking*. Macmillan, New York, p. 395.

45 Burkhardt, R. 2007. *A Technology for Designing Tensegrity Domes and Spheres* <http://bobwb.tripod.com/prospect/prospect.htm>

46 Cavendish, H. 'Experiments to determine the Density of the Earth', *Philosophical Transactions of the Royal Society of London*, (part II) **88** p.469-526 (21 June 1798), reprinted in Cavendish 1798.